

MR Travel to Scan Image Processing for Real-Time Liver Identification

S. P. Dries¹, D. Bystrov¹, V. Pekar², H. S. Heese¹, P. Koken¹, J. Keupp¹, and P. Börnert¹

¹Philips Research Europe, Hamburg, Germany, ²Philips Research North America, Markham, Ontario, Canada

Introduction

Continuously moving table whole body MR^{1,2,3,4} survey scanning can be performed uninterruptedly while the patient is moved into the system until the organ or other region of interest arrives in the iso-center (travel-to-scan). For the purpose of subsequent automated scan geometry planning⁵, it is important to segment the region of interest automatically from the survey data. The method described herein automatically estimates the position of the patient's liver in continuously acquired 3-D survey data. The detection algorithm is aimed to give feedback to the scanner on-the-fly when the liver is detected and provide its position and extent, i.e. to stop the table. The specific requirements, apart from robustness of the method, include a real-time constraint and the capability of dealing with partitions of the image data.

Method

Three cascaded processing steps are implemented as a callback routine. The image data is passed to the routine after the acquisition of each consecutive stack of approximately 20 slices in real-time. If the liver has been detected the program returns the longitudinal (feet-head) extent of the liver and a 3-D shape model representing the actual liver volume in the image data. Ten continuously moving table whole body volunteer scans were used that were all acquired head first, supine with 36mm/s bed speed at an isotropic voxel size of 5.4³mm³ in a volume of 96×56×360 voxels.

The first processing step is sampling of the image data in the longitudinal direction. If the liver area can be estimated from that, the upper and lower z-boundaries are derived. As a second step, x- and y-axis sampling is added. This yields an estimated center of the liver in 3-D. In the third step an active shape model is positioned and adapted locally by energy minimization⁶.

1. z-sampling (extent along longitudinal axis): After thresholding to reduce background noise, for each transverse slice a signal weighted center of gravity is determined. Four histograms and their first and second derivatives are calculated from four sectors that are defined by the centers of gravity as origin and two straight lines $y=x$ and $y=-x$ subdividing each slice. These histograms serve as image features that are used to segment the longitudinal extent of the liver. For each sector of each slice a histogram value is calculated by averaging the gray values of the voxels multiplied by their Euclidean distance from the center. The histogram curves for each of the four sectors are then smoothed by convolving them with a Gaussian, and their first and second derivatives are calculated by convolving them with a first or second order Gaussian derivative, respectively (Figure 1).

From the ten test datasets, a model was derived experimentally that allowed the estimation of the liver boundary. The model comprises the sigma and the size of the Gaussian kernel that constrain the amount of smoothing as well as conserved features like minima, maxima, roots or ratios.

2. (x,y)-sampling (center in transverse plane): Between the estimates of the upper and lower liver boundary the image is sampled in y- (sagittal) and x- (transverse) axes in a slice averaged from the five central slices (estimated and smoothed middle transverse plane through the liver), starting from its center of gravity analogously to z-sampling but with different sigma. After this step a 3-D bounding box of the estimated liver area is defined and its center is used to pre-position the active shape model.

3. Active shape model adaptation (3-D volume localization): An active shape model of the liver is locally adapted to the image data by an algorithm⁶ described previously that takes displacement, deformation and strength of the gray value gradients found in the image into account. It adapts the model by minimizing iteratively the sum of the internal (shape preserving) and external (deforming) energies. The adapted model indicates the location, shape and orientation of the liver in the patient data (Figure 2).

Results

The detection of the superior and inferior margins of the liver was compared numerically to a ground truth manual segmentation of the most superior and most inferior points of the liver.

The results of the histogram-based initial automated detection (z-sampling) and of the subsequent shape model adaptation, reduced to the superior-most and inferior-most vertices of the mesh, were used for evaluation. The deviations are given in millimeters by descriptive statistics for automated z-sampling and automated shape model adaptation (Table).

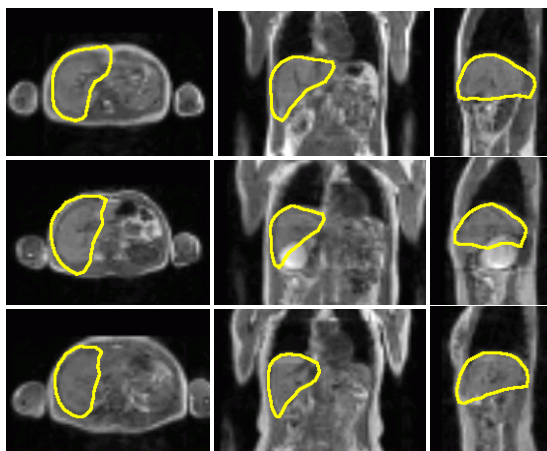


FIGURE 2: Visualization of active shape model adaptation. For three different volunteers (rows) in different orientations: transverse, coronal and sagittal (columns), the found liver boundaries are superimposed in yellow.

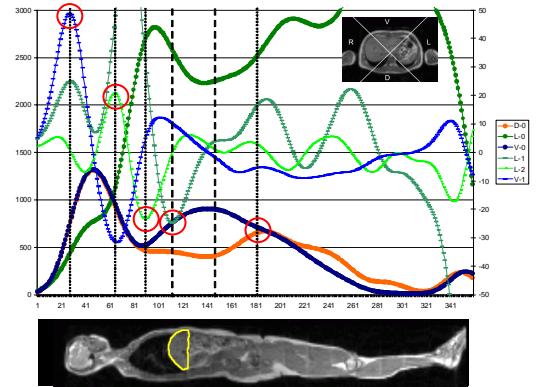


FIGURE 1: The plot shows the relevant histograms (dorsal (D), left (L), and ventral (V) sectors (insert), -0) and first (-1) and second (-2, scaled ×5) derivatives versus the z-axis for one volunteer. Vertical black lines with red circles indicate experimentally derived features for z-sampling, liver margins dashed. A sagittal slice from the volunteer 3-D dataset is aligned below. Note that the inferior liver margin is laterally to the slice shown.

n=10	deviation {upper, lower} / mm		computation time / s
	z-sampling	3-D shape model	
mean±sd	21±16	2±2	1,7±0,1
(min-max)	(1-48)	(0-5)	(1,6-2,0)

Discussion

The presented method robustly segmented the liver region from ten test cases. Although testing was done on volunteer and not on patient data, variability as shown in Fig. 2 was accommodated with constant parameters of the entire model.

Numerical evaluation showed correct identification of the superior liver margin after model based segmentation, which is attributable to the strong intensity gradient between the lung and the liver. Identification of the inferior margin was less accurate, which is attributable to the weaker gradient between the liver and adjacent abdominal organs. The initial estimation from z-sampling that had errors of about 4 (superior) and 7 (inferior) voxels on average was improved by model based segmentation to 0 and 4 voxels, respectively. For the envisioned application this is a negligible source of error: automated planning of diagnostic scan geometries would be sufficiently enabled by the 3-D segmentation that results from the presented method. The rationale for introducing the comparatively complex method of active shape models is to not only allow for a table-stop signal but to use the travel-to-scan data already as survey scan for subsequent automated scan planning.

Overall computation time was no limit for on-the-fly calculation during scan acquisition that takes about 20–30s to reach the liver.

References

- Bojahr O, Holz D, Rasche V, et al.; Proc. ISMRM 4: 1734, 1996
- Shankaranarayanan A, Brittain J; Proc ISMRM 12: 103, 2004
- Kruger DG, Riederer SJ, Grimm RC, et al.; Magn Reson Med 47: 224–231, 2002.
- Aldefeld B, Börnert P, and Keupp J; Magn Reson Med 55: 1210–1216, 2006
- Young S, Bystrov D, Netsch T, et al.; Proc. ISMRM 14: 1588, 2006
- Weese J, Kaus M, Lorenz C, et al.; Proc. IPMI: 380–387, 2001